Helmke and Heald, http://www.jcb.org/cgi/content/full/jcb.201401014/DC1

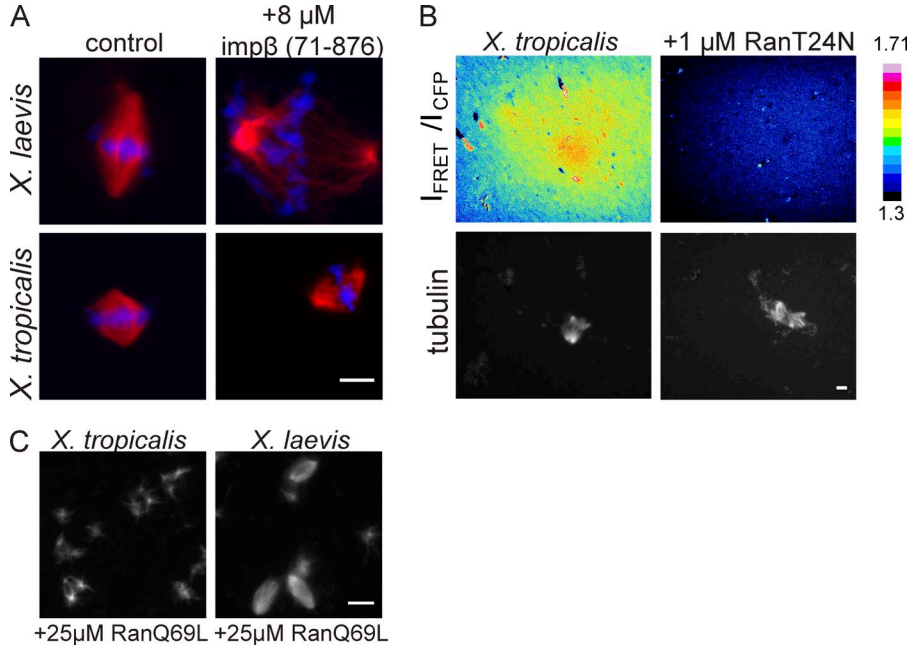

Figure S1. ***X. tropicalis* and *X. laevis* spindles differ in their requirement for the RanGTP pathway.** (A) Inhibition of the RanGTP pathway with 8 µM of the importin β cargo-binding domain (71–876) disrupted spindle assembly in *X. laevis* but not *X. tropicalis* egg extracts. Bar, 10 µm. (B) Visualization of RanGTP gradient in *X. tropicalis* spindles using 1 µM of the Rango FRET probe (Kaláb et al., 2006). FRET efficiency shown by I_{FRET}/I_{CFP}. 1-µM RanT24N treatment abolished this gradient, but spindle assembly still occurred, as seen by the presence of MT structures. Bar, 10 µm. (C) Treatment of *X. laevis* and *X. tropicalis* egg extracts with 25 µM RanQ69L induced ectopic MT nucleation in both reactions, but MT organization into bipolar arrays was not observed in *X. tropicalis*. Bar, 10 µm.

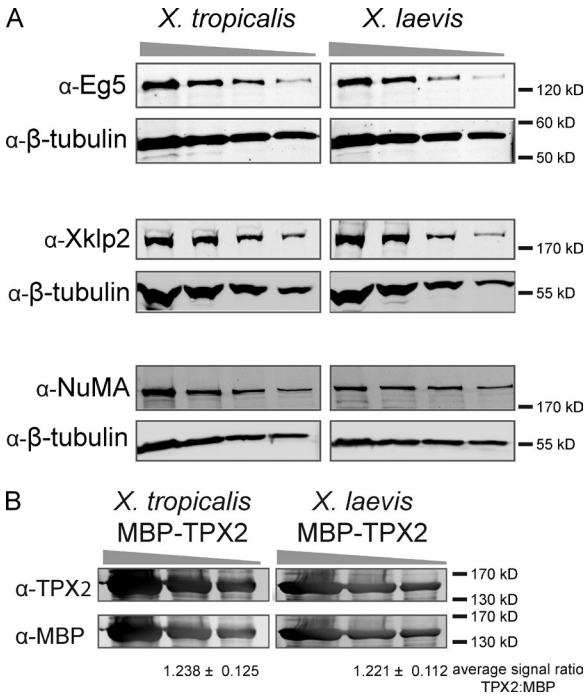

Figure S2. **Concentration comparison of spindle assembly factors in *X. tropicalis* and *X. laevis*.** (A) Representative Western blots of a dilution series of *X. tropicalis* and *X. laevis* egg extract probed for each of the indicated factors. β-Tubulin is shown as a loading control for each gel. Eg5, Xklp2, and NuMA showed similar concentrations in both extracts. (B) Representative Western blot of dilution series of recombinant *X. tropicalis* MBP-TPX2 and recombinant *X. laevis* MBP-TPX2, probed with the TPX2 antibody shown in B as well as an α-MBP antibody. Band intensities were quantified (Odyssey software) and the signal ratio of TPX2/MBP was calculated for each lane. The signal ratios were not significantly different: 1.238 ± 0.125 in *X. tropicalis* and 1.221 ± 0.112 in *X. laevis*.

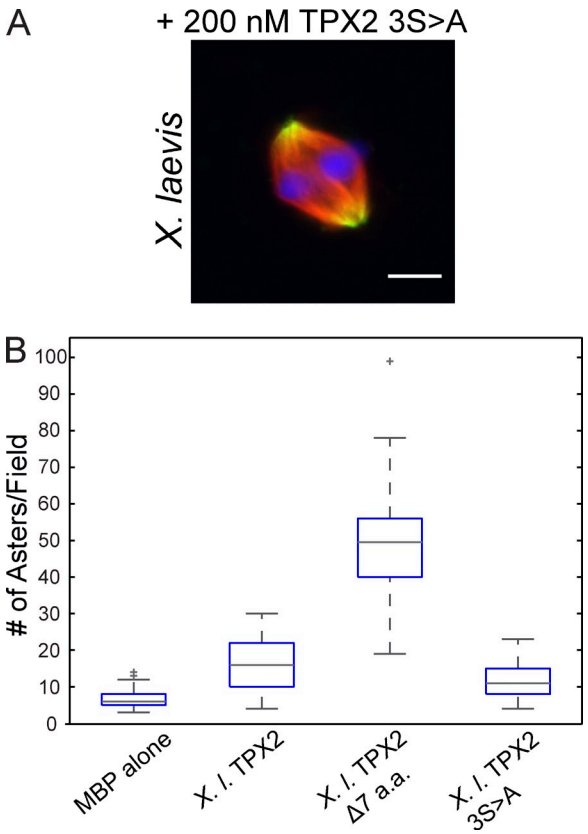

Figure S3. **Phospho-null mutant of *X. laevis* TPX2 does not show altered MT nucleation activity.** (A) Spindle morphology upon addition of phospho-null mutant of *X. laevis* TPX2 (S218A, S220A, and S222A) to *X. laevis* extract. Recombinant protein did not induce MT aster formation at spindle poles, similar to WT *X. laevis* TPX2. Bar, 10 μm. (B) Nucleation measured by asters per field (outliers indicated by +) shows phospho-null mutant behaved like WT *X. laevis* TPX2 and not like the *X. laevis* Δ7 mutant. Boxplot of number of asters per field with median marked by gray line, first and third quartiles marked by box edges, and data maxima and minima noted by whiskers.

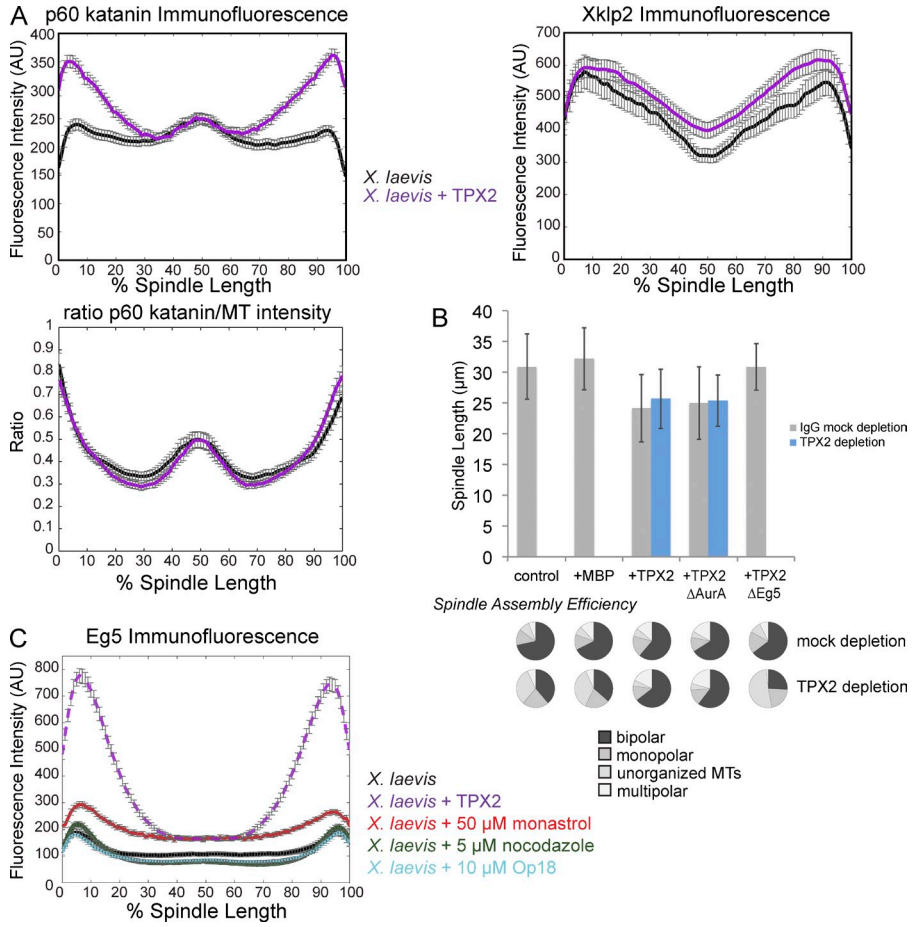

Figure S4. **TPX2 addition does not significantly affect Xklp2 or katanin, but specifically alters Eg5 localization, and its effects require the C-terminal Eg5-binding domain in TPX2-depleted extracts.** (A) Line scan quantification of p60 katanin or Xklp2 immunofluorescence intensity in *X. laevis* spindles with and without addition of recombinant TPX2 to 200 nM. Spindle lengths were normalized for statistical analysis. Mean ± standard error; $n \geq 90$ spindles for each condition from three extracts for p60 staining and $n \geq 42$ spindles for each condition from two extracts for Xklp2 staining. Although p60 katanin localization increased slightly at the poles, comparing the katanin signal to MT intensity shows that the ratio of p60/MT remained unchanged. Xklp2 staining was not altered with TPX2 addition. (B) Quantification of spindle length after addition of TPX2 mutants to egg extracts immunodepleted of endogenous TPX2. Gray bars indicate mock depletion with IgG and blue bars indicate TPX2 depletion. Depletion of TPX2 disrupted spindle assembly efficiency and spindle morphology, illustrated by percentage in bottom panels (calculated in >300 structures for each condition in three separate extracts). TPX2ΔAurA rescued both spindle assembly and reduced spindle length similarly to full-length TPX2. TPX2ΔEg5 did not rescue spindle assembly efficiency. Spindle length was not quantified in TPX2 depletion conditions (control, +MBP, and +TPX2ΔEg5) because spindle morphology and assembly were severely impaired. (C) Line scan quantification of Eg5 immunofluorescence intensity in *X. laevis* spindles after treatment with 10 µM Op18, 5 µM nocodazole, or 50 µM monastrol. Nocodazole and Op18, which both reduce spindle size, resulted in little change in Eg5 localization. Monastrol, which inhibits Eg5 motor activity, increased Eg5 staining slightly along the length of the spindle. In comparison, addition of TPX2 (data from Fig. 4 D) caused significant polar recruitment of Eg5 to the spindle. Mean ± standard error; $n \geq 60$ spindles for each condition from two extracts.

Reference

Kaláb, P., A. Pralle, E.Y. Isacoff, R. Heald, and K. Weis. 2006. Analysis of a RanGTP-regulated gradient in mitotic somatic cells. *Nature*. 440:697–701. http://dx.doi.org/10.1038/nature04589